

Highlights

- Electrochemical degradation and mineralization of perfluorooctanoic acid is achieved
- Novel ultrananocrystalline boron doped conductive diamond electrode is applied
- Increasing the applied current density enhanced the kinetics of PFOA mineralization
- Hydroxyl radical formation is related to the kinetics of PFOA degradation

22 **Kinetics of the electrochemical mineralization of perfluorooctanoic**
23 **acid on ultrananocrystalline boron doped conductive diamond**
24 **electrodes**

25
26
27 **Abstract**

28 This work deals with the electrochemical degradation and mineralization of
29 perfluorooctanoic acid (PFOA). Model aqueous solutions of PFOA (100 mg/L) were
30 electro-oxidized under galvanostatic conditions in a flow-by undivided cell provided
31 with a tungsten cathode and an anode formed by a commercial ultrananocrystalline
32 boron doped diamond (BDD) coating on a niobium substrate. A systematic
33 experimental study was conducted in order to analyze the influence of the following
34 operation variables: i) the supporting electrolyte, NaClO₄ (1.4 and 8.4 g/L) and Na₂SO₄
35 (5 g/L); ii) the applied current density, j_{app} , in the range 50-200 A/m² and iii) the
36 hydrodynamic conditions, in terms of flowrate in the range 0.4×10^{-4} - 1.7×10^{-4} m³/s and
37 temperature in the range 293-313 K. After 6 hours of treatment and at j_{app} 200 A/m²,
38 PFOA removal was higher than 93% and the mineralization ratio, obtained from the
39 decrease of the total organic carbon (TOC) was 95%. The electrochemical generation of
40 hydroxyl radicals in the supporting electrolyte was experimentally measured based on
41 their reaction with dimethyl sulfoxide. The enhanced formation of hydroxyl radicals at
42 higher j_{app} was related to the faster kinetics of PFOA removal. The fitting of
43 experimental data to the proposed kinetic model provided the first order rate constants
44 of PFOA degradation, k_c^1 that moved from 2.06×10^{-4} to 15.58×10^{-4} s⁻¹, when j_{app} varied
45 from 50 to 200 A/m².

46
47
48 **Keywords**

49 perfluorooctanoic acid, ultrananocrystalline boron doped diamond anode,
50 electrochemical oxidation, perfluoroalkyl substances, hydroxyl radicals

52 **1. Introduction**

53 Among emerging water contaminants, perfluoroalkyl substances (PFASs) are
54 particularly problematic because they are highly persistent, bio-accumulative and have
55 been detected ubiquitously in the abiotic environment, biota, food items and humans, all
56 over the planet (Cornelis et al., 2012; Johanson et al., 2014). PFASs exhibit the special
57 physical-chemical characteristics of chemical and thermal stability, low surface free
58 energy and surface active properties (Lehmler, 2005). These features have promoted
59 their utilization as water and oil repellents, fire retardants, reactants in polyurethane
60 production and vinyl polymerization, herbicide and insecticide formulations, cosmetics,
61 greases and lubricants, paints, polishes and adhesives. The wide-spread use of PFAS has
62 resulted in an important release of these compounds into the environment, which was
63 estimated at 3200-7300 tons during the period 1950-2004 by direct and indirect
64 emissions (Prevedouros et al., 2006).

65 Among the PFASs, perfluorooctanesulfonate (PFOS) and perfluorooctanoic acid
66 (PFOA), are subjected to increasingly intense research. Taking into account their
67 potential toxicity and the extent of their environmental distribution, these compounds
68 have started to be regulated by various international bodies. PFOS is part of the OSPAR
69 List of Chemicals for Priority Action (Ospar, 2011). PFOS and its salts are also
70 included in the Annex B of the Stockholm Convention on Persistent Organic Pollutants
71 (Stockholm-Convention-Secretariat, 2009) and it has been included as a priority
72 substance in the field of European water policy according to Directive 2013/39/EC.
73 PFOA is still produced and used, however it is listed in the Candidate List of
74 Substances of Very High Concern under the European regulation REACH (ECHA,
75 2013).

76 The scientific community is facing the challenge of developing clean technologies for
77 the treatment at source of the emissions of PFASs and for the abatement of the existing
78 water polluted sites. Among others, literature reports the use of membrane (Thompson
79 et al., 2011), adsorption (Carter and Farrell, 2010; Eschauzier et al., 2012) and/or ion
80 exchange processes (Ochoa-Herrera and Sierra-Alvarez, 2008; Xiao et al., 2012).
81 However, these technologies imply the transfer of the contaminants to a second phase
82 and the generated waste must be managed in order to avoid the impact of its disposal on
83 the receiving environment.

84 The destructive methods aim at the cleavage of the C-F bonds to form F⁻ ions. The
85 electrochemical oxidation is a technology that has demonstrated its capacity to degrade
86 refractory organic contaminants such as emerging contaminants contained in the
87 secondary effluents of wastewater treatment plants (Pérez et al., 2010; Urriaga et al.,
88 2013), polychlorinated dibenzo-p-dioxins and dibenzofurans (Vallejo et al., 2013) and
89 organic pollutants in industrial wastewaters (Urriaga et al., 2014). Electro-oxidation is
90 presented as a clean alternative since its main reactants are electrons. Furthermore,
91 robustness, versatility and the easy automation are other advantages (Anglada et al.,
92 2009). The anodic material plays a key role, and previous studies have shown the
93 effectiveness of boron doped diamond (BDD), SnO₂ and PbO₂ in the degradation and
94 mineralization of perfluorocarboxylic and perfluorosulfonic acids (Ochiai et al., 2011;
95 Zhuo et al., 2011; Zhao et al., 2013; Lin et al., 2012; Carter and Farrell, 2008; Niu et al.,
96 2012) in model solutions. Whereas the use of electrodes based on tin and lead can be
97 questioned because of the leaching of these toxic metals into the treated waters, the
98 stability and effectiveness of boron doped diamond electrodes make this material an
99 excellent candidate for the effective degradation of PFASs in contaminated waters
100 (Xiao et al., 2011; Zhuo et al., 2012). So far, the effect of electro-oxidation parameters

101 on the PFASs degradation ratio has not been considered in depth and controversial
102 results are found for the studied variables namely, current density, electrolyte solution,
103 pH, initial compound concentration, background electrolyte, temperature and fluid-
104 dynamics. Although some researchers (Lin et al., 2012; Niu et al., 2012, 2013; Ochiai et
105 al., 2011; Zhao et al., 2013; Zhuo et al., 2011) have studied the degradation mechanisms
106 of PFOA, no final pathway is stated.

107 Usually, BDD electrodes are composed of a boron doped microcrystalline diamond
108 rough film with relatively large grain size (0.5-10 μm) that can contain pinholes and
109 defects (Chaplin et al., 2011). The thickness of the diamond film needs to be of several
110 microns to reduce the number of pinholes (Gruen, 2006). Some examples of
111 microcrystalline BDD commercial electrodes can be found in previous electro-oxidation
112 studies of PFASs (Fryda et al., 2003; Liao and Farrell, 2009).

113 In the present study a new ultrananocrystalline boron doped conductive diamond
114 (UNCD) electrode provided with a thin film coating and nanoscale grain size was tested
115 in the electro-oxidation of perfluorooctanoic acid. Towards that end, a commercial
116 electro-oxidation flow-by undivided cell was used. The influence of the main process
117 variables on the PFOA degradation kinetics, i.e.: applied current density, electrolyte
118 composition, recirculation flow rate and temperature, the mineralization degree and the
119 fluoride generation, is presented. Moreover, the generation of oxidant species, e.g.:
120 hydroxyl radicals and hydrogen peroxide, is related to the process variables and to the
121 kinetic analysis of PFOA degradation.

122 **2. Materials and Methods**

123 *2.1. Materials*

124 All chemicals used in the experiments were reagent grade or higher and were used as
125 received without further purification. Perfluorooctanoic acid (PFOA) (96%) was
126 purchased from Sigma Aldrich Chemicals. Dihydrogen phosphate (99%), sodium sulfate
127 (99%) and methanol were obtained from Panreac (Spain), while sodium perchlorate
128 monohydrate (98%) was purchased to Merck. PFOA was dissolved in ultrapure water
129 (Q-POD Millipore) to prepare feed solutions with an initial concentration of 100 mg/L
130 (0.24 mol/m^3). Sodium perchlorate 1.4 and 8.4 g/L (10 mol/m^3 and 60 mol/m^3) and
131 sodium sulfate 5 g/L (35.2 mol/m^3) were used as electrolytes.

132 *2.2 Electrochemical experiments*

133 Figure 1 shows a diagram of the experimental set-up used in the electro-oxidation
134 experiments. It consisted of a tank in which the feed solution was stored before it started
135 to circulate through the electrolytic cell by means of a magnetic pump. All experiments
136 were carried out in discontinuous mode, i.e. the PFOA solution was continuously
137 circulated from the reservoir to the cell and back to the tank in a closed loop. The
138 recirculation flowrate was set at $1.11 \times 10^{-4} \text{ m}^3/\text{s}$, unless otherwise stated. The
139 temperature was maintained at $293 \pm 2 \text{ K}$ by circulating a cooling fluid through the
140 jacket of the feed tank, unless otherwise stated. The single compartment electrochemical
141 cell (Diamonox 40) was supplied by Advanced Diamond Technologies (Romeoville,
142 U.S.A.). The cell is comprised of two rectangular electrodes disposed in parallel with a
143 surface area of $42 \times 10^{-4} \text{ m}^2$ each. The anode is made of a boron doped
144 ultrananocrystalline diamond (UNCD) coating (2 μm film thickness and 3-5 nm of
145 average grain size) on a niobium substrate while tungsten was employed as cathodic
146 material. The distance between electrodes was $8 \times 10^{-3} \text{ m}$. The electric power required
147 during the electro-oxidation experiments was provided by a laboratory power supply

148 (75-H-Y3005D Vitrico) with a maximum output of 5 A and 30 V. The experiments
149 were performed at constant current density. Samples were withdrawn from the feed tank
150 at regular time intervals and preserved in the refrigerator at 4 °C until analysis.

151 *2.3. Analytical methods*

152 The concentration of PFOA was determined using a HPLC-DAD system (Waters 2695)
153 equipped with a X Bridge C18 column (5µm, 250 mm x 4.6 mm, Waters) and UV-
154 Visible spectrophotometric detector. The separation column was set in an oven at 40 °C.
155 A mixture of methanol (65%) and di-hydrogen phosphate (35%) was used as mobile
156 phase in an isocratic mode with a flow rate of 0.5 ml/min. The variable wavelength of
157 the detector was set at 204 nm. The limit of quantification was 7.4 mg/L.

158 TOC analyses were performed using a TOC-V CPH (Shimadzu). The concentration of
159 fluoride ion was measured by ion chromatography using an ICS-1100 system (Dionex)
160 equipped with an IonPac-AS9HC column and a conductivity detector. A solution of
161 sodium carbonate (9 mol/m³) was used as mobile phase and the flow rate was set at 1
162 mL/min.

163 The determination of hydrogen peroxide was performed by using a specific kit,
164 Merckoquant Peroxide Test (118789 Spectroquant), suitable for determining H₂O₂
165 concentrations in the range 0.0001 - 0.18 mol/m³. The method for the hydroxyl radicals
166 determination was adapted from Tai et al. (2004). The method is based on the reaction
167 between hydroxyl radicals and dimethyl sulfoxide to produce formaldehyde
168 quantitatively, which then reacts with 2,4-dinitrophenylhydrazine (DNPH) to form the
169 corresponding hydrazone that is finally analyzed by HPLC-UV.

170 **3. Results and discussion**

3.1. Influence of the electrolyte

Preliminary experiments were performed in order to select an adequate supporting electrolyte. Previous studies (Zhuo et al., 2012; Ochiai et al., 2011; Liao and Farrell, 2009) reported the use of sodium perchlorate as it is an inert compound towards oxidation at conductive diamond electrodes. Fig. 2a shows the evolution of PFOA concentration with the electrolysis time for two different concentrations of sodium perchlorate, 1.4 and 8.4 g/L. The measured conductivities of the two initial solutions were 0.11 and 0.57 Sm^{-1} , respectively. A small, although significant increase of the PFOA degradation kinetics is observed at the lowest electrolyte concentration. This positive kinetic effect could be related to the higher cell voltage, depicted in Fig. 2b, obtained as a consequence of the lower conductivity of the electrolyte, which is inversely proportional to the system resistance and according to the Ohm's law, a higher voltage is expected. Although the anode voltage could not be directly measured in this type of experimental set-up, it is hypothesized that at the higher cell voltage obtained for sodium perchlorate 1.4 g/L, the electrode voltage was also higher and the oxidation potential was increased, resulting in the observed increase of the PFOA degradation rate. However, NaClO_4 should be avoided in the treatment of real wastewaters, since this compound is considered as a contaminant itself, that is, perchlorate may have an adverse effect on the health of persons (EPA, 2011). Sodium sulfate is a safer electrolyte that is widely employed in the electrochemical practice (Niu et al., 2013; Xiao et al., 2011; Zhao et al., 2013). Fig. 2a compares the degradation of PFOA using sodium sulfate (5 g/L) and sodium perchlorate (8.4 g/L) as electrolytes. The conductivity of the initial sodium sulfate solution was 0.63 Sm^{-1} . It is observed that PFOA degradation rates were not influenced by the type of electrolyte, as the experimental trends of concentration and voltage are practically overlapped. Moreover,

196 PFOA electro-oxidation kinetics were not enhanced by the use of sulfate as electrolyte,
197 thus it is concluded that at the conditions applied in the present study, the use of sodium
198 sulfate did not promote the generation of secondary oxidants that could contribute to the
199 degradation of PFOA.

200 *3.2. Influence of the applied current density*

201 The effect of the applied current density on the degradation rates of PFOA was
202 investigated in the range of j_{app} values of 50, 100 and 200 A/m². Experimental data of
203 the change of PFOA, TOC and fluoride concentrations are shown in Fig. 3. It is
204 observed that the kinetics of PFOA degradation was significantly enhanced when
205 increasing the applied current density from 50 to 100 A/m², although the effect of a
206 further increase of j_{app} to 200 A/m² was less significant.

207 The influence of current density on the electro-oxidation of PFASs on conductive
208 diamond electrodes has been previously studied by several authors, with differing
209 conclusions. Zhuo et al. (2012) reported the PFOA degradation (50 mg/L) on non-
210 commercial Si/BDD; the authors observed that the applied current density in the range
211 5.9-58.8 A/m² exerted a small influence on the first order degradation rate; similar
212 outcomes were found by Carter & Farrell (2008) when dealing with the degradation of
213 perfluorooctane sulfonate (PFOS) using commercial BDD anodes purchased to
214 Adamant Technologies in the range $10 < j_{app} < 200$ A/m², although they observed zeroth
215 order PFOS degradation kinetics. On the contrary, Ochiai et al. (2011) showed that
216 PFOA removal using commercial BDD anodes obtained from Condias was enhanced at
217 higher j_{app} , although the decomposition rate was saturated for current densities over 6
218 A/m²; Liao & Farrell (2009) also reported that the perfluorobutane sulfonate (PFBS)

219 electro-oxidation rates were enhanced at increasing values of j_{app} in the range 5-200
220 A/m².

221 TOC was measured as an indicator of PFOA mineralization. Fig. 3b shows that TOC
222 decreased in a similar manner as PFOA concentration did. However, TOC evolution is
223 slightly slower than PFOA degradation, and the effect of the applied current density is
224 more significant when changing j_{app} from 100 to 200 A/m², as it also happens in the
225 generation of fluoride anions (Fig. 3c). This is an evidence of the formation of
226 intermediate oxidation products, smaller perfluorocarboxylic compounds (Lin et al.,
227 2013). Nevertheless, at $j_{app} = 200$ A/m² the low values of TOC obtained after 6 hours of
228 treatment indicate that electro-oxidation with UNCD anode succeeds to mineralize
229 PFOA.

230 To evaluate the effectiveness of the treatment in terms of PFOA mineralization, the
231 mineralization index (M.I.) was defined (Eq. 1),

$$M.I. = \frac{\Delta TOC_{exp}}{\Delta TOC_{calculated\ from\ PFOA}} \cdot 100 = \frac{TOC_{exp,0} - TOC_{exp,t}}{TOC_{c,0} - TOC_{c,t}} \cdot 100 \quad (Eq. 1)$$

232 where TOC_{exp} is the experimental value of TOC and TOC_c is the value of TOC
233 calculated from the concentrations of PFOA. The subscripts 0 and t refer to the initial
234 value and to the value at a given experimental time, respectively. The values of M.I.
235 obtained during the course of the electro-oxidation experiments for the different applied
236 current densities are listed in Table 1. It is shown that increasing the applied current
237 density and the electrolysis time provided an increase in the values of the M.I. of PFOA,
238 ranging from 55.8 to 94.9% for 50 and 200 A/m², respectively after 6 hours of
239 experiment. This indicates the successful conversion of PFOA into CO₂ and can be

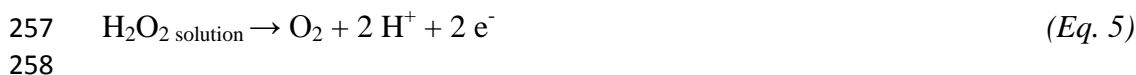
240 explained due to the enhanced formation of hydroxyl radicals at higher current densities
241 (Kapalka et al., 2008).

242 It has been referenced (Michaud et al., 2003) that the first step of water oxidation on
243 conductive diamond anodes is the formation of hydroxyl radicals (Eq. 2),



245 In this work, the generation of hydroxyl radicals at different applied current densities
246 was measured. Duplicate experiments (S.D. < 5%) were performed in the absence of
247 PFOA, and the average results are shown in Fig. 4a. It is observed that the increase in
248 the applied current density enhanced the formation of hydroxyl radicals.

249 According to Michaud et al. (2003) the electro-generated hydroxyl radicals can be
250 involved in four parallel reactions:(i) Oxidation of supporting electrolyte; ii) O₃
251 formation, iii) BDD combustion and (iv) H₂O₂ formation, electro-generated hydroxyl
252 radicals may react with each other forming hydrogen peroxide near the electrode (Eq.
253 3); this then diffuses into the bulk of the electrolyte (Eq. 4) or is oxidized to oxygen (Eq.
254 5),



259 Figure 4b shows the trend of H₂O₂ concentration in the electrolyte during electrolysis in
260 Na₂SO₄ at the three values of the applied current density, j_{app} 50, 100 and 200 A/m².
261 The set of reactions (Eqs. 2-5) explains both the presence of hydrogen peroxide in the

262 electrolyte and the trend of its concentration towards a limiting value that was
263 comprised in the range 0.060-0.070 mol/m³.

264 3.3. Effect of the flowrate and temperature

265 In order to analyze the influence of the hydrodynamic conditions on the kinetics of
266 PFOA removal, the effects of varying the feed flowrate in the range 0.4×10^{-4} - 1.7×10^{-4}
267 m³/s and temperature in the range 293-313 K were experimentally studied (Fig. SM-1
268 and Fig. SM-2 in Supplementary Material (SM)). Even though the Reynolds number
269 changed from the laminar regime when operating at the lowest flowrate ($Re = 1371$) to
270 the turbulent regime at the highest flowrate ($Re = 5894$) no significant effect was
271 observed either in the removal of PFOA or in the generation of fluoride. Similarly, the
272 effect of changing the process temperature in the studied range did not exert any
273 influence on the evolution of both response variables. This behavior indicates that the
274 kinetics of PFOA degradation by electro-oxidation with UNCD anodes is not limited by
275 mass transfer, regardless the low concentrations employed in the present work.

276 3.4. Kinetic analysis

277 The mass balances for the concentration of PFOA applied to the two main elements of
278 the experimental system are written as follows,

279 Electro-oxidation cell

$$\frac{\partial C_a}{\partial t} = -\frac{Q}{A} \cdot \frac{\partial C_a}{\partial z} - r_a \quad (\text{Eq. 6})$$

280 Recirculation feed tank

$$V \cdot \frac{dC_{out}}{dt} = Q \cdot C_{a_{in}} - Q \cdot C_{a_{out}} \quad (\text{Eq. 7})$$

281 Where Q is flow-rate (m^3/s), V is the volume of treated dissolution (m^3), A is the cross
 282 section of the fluid circulation channel ($A= d \cdot M$, m^2), C_a is the PFOA concentration
 283 (mol/m^3), r_a is the reaction rate of the electro-oxidation process ($\text{mol}/\text{m}^3/\text{s}$), z is the axial
 284 position along the cell and t is time (s).

285 Several assumptions were made for the integration of the mass balances. Firstly, it was
 286 considered that in the electro-oxidation cell the variation with time of PFOA
 287 concentration was negligible compared to its variation along the axial position $\frac{\partial C_a}{\partial t} \ll$
 288 $\frac{\partial C_a}{\partial z}$, and $\frac{\partial C_a}{\partial t} = 0$. Secondly, first order kinetics is considered for the electro-oxidation
 289 process, Eq. (8)

$$r_a = k_c^1 \cdot C_a \quad (\text{Eq. 8})$$

290 where k_c^1 is the kinetic constant (s^{-1}). Then Eq. (6) was integrated along the cell length
 291 (from $z=0$ to $z=L$) and substituted into Eq. (7) by means of Eq. (9) and Eq. (10),

$$C_{a_{z=L}} = C_{a_{in}} \quad (\text{Eq. 9})$$

$$C_{a_{z=0}} = C_{a_{out}} \quad (\text{Eq. 10})$$

292 The resulting mass balance was integrated between the beginning of the experiment
 293 ($t=0$) and a certain time t . The final integrated equations is presented in Eq. (11),

$$V \cdot \ln\left(\frac{C_{a_0}}{C_a}\right) = Q \cdot \left[1 - \exp\left(-\frac{k_c^1 V^{cell}}{Q}\right)\right] t \quad (\text{Eq. 11})$$

294 The experimental data of PFOA development given in Fig. 3 were satisfactorily fitted to
 295 Eq. (11) as it is shown in Fig. 5. A summary of the results is presented in Table 2. The
 296 observed values of the kinetic constant k_c^1 were compared to the mass transport

297 coefficient (k_m) calculated for the mass transfer of PFOA through the liquid boundary
298 layer within the cell. A standard correlation (Perry, 2007), Eq. (12), for Newtonian
299 fluids circulating in closed channels, was applied,

300 Turbulent flow regime ($2000 < Re < 35000$) $Sh = 0.023 \cdot Re^{0.83} \cdot Sc^{0.44}$ (Eq. 12)

301 where Sh , Re and Sc are the Sherwood number, Reynolds number and Schmidt number,
302 respectively. Water density and viscosity were used to calculate the diffusion coefficient
303 according to the Wilke-Chang correlation for diffusion of organic compounds in liquids
304 (Perry, 2007), and the obtained value was $5.1 \times 10^{-10} \text{ m}^2 \text{ s}^{-1}$. Taking into account the
305 surface to volume ratio of the electrochemical cell ($A/V = 8.4 \text{ m}^{-1}$), the k_m value for the
306 experiments performed at $Q = 1.11 \times 10^{-4} \text{ m}^3/\text{s}$ would correspond to a kinetic constant of
307 $2.02 \times 10^{-4} \text{ s}^{-1}$. The value of k_c^I obtained at $j_{app} = 50 \text{ A/m}^2$ is $2.06 \times 10^{-4} \text{ s}^{-1}$, that is very
308 close to the theoretical value derived from k_m . Increasing the applied current densities
309 results in values of the apparent kinetic constant of $8.63 \times 10^{-4} \text{ s}^{-1}$ (at $j_{app} = 100 \text{ A/m}^2$) and
310 $15.58 \times 10^{-4} \text{ s}^{-1}$ (at $j_{app} = 200 \text{ A/m}^2$). The difference is assigned to the enhanced secondary
311 oxidation processes in the bulk derived from the higher concentration of electro-
312 generated oxidants at higher current densities. This excludes mass transport limitations
313 in the experimental system. At the same time, the enhancement of PFOA electro-
314 oxidation kinetics by higher applied current densities points to the higher generation of
315 hydroxyl radicals and supports the mechanism that involves the role of hydroxyl
316 radicals in PFOA degradation.

317 **4. Conclusions**

318 This work presents an experimental study on the electrochemical treatment of
319 perfluorooctanoic acid (PFOA) in aqueous solutions using a novel commercial

320 ultrananocrystalline boron doped diamond anode. The following conclusions can be
321 withdrawn:

322 1. PFOA degradation and mineralization ratios higher than 90% were easily achieved.

323 2. First order PFOA degradation rates were observed. The operating variable that
324 exerted the most positive kinetic effect was the applied current density.

325 3. Increasing the applied current density positively influenced on the hydroxyl radical
326 generation in the electrochemical system. At the same time, the kinetic analysis of the
327 system showed that PFOA degradation rate was not limited by mass transfer. Therefore
328 it was concluded that hydroxyl radicals play a predominant role in PFOA degradation
329 using ultrananocrystalline BDD electrodes.

330 It is concluded that electro-oxidation with BDD anodes is a promising technology for
331 the treatment of perfluoroalkyl substances in polluted waters.

332 **Appendix A. Supplementary material**

333 Supplementary data on the kinetic evolution of PFOA and fluoride concentrations at
334 variable flowrate and temperature are included.

335 **References**

- 336 • Anglada, A., Urtiaga, A., Ortiz, I., 2009. Contributions of electrochemical oxidation
337 to waste-water treatment: fundamentals and review of applications. *J. Chem.*
338 *Technol. Biot.* 84, 1747-1755.
- 339 • Carter, K. E., Farrell, J., 2008. Oxidative destruction of perfluorooctane sulfonate
340 using boron-doped diamond film electrodes. *Environ. Sci. Technol.* 42, 6111-6115.

- 341 • Carter, K. E., Farrell, J., 2010. Removal of perfluorooctane and perfluorobutane
342 sulfonate from water via carbon adsorption and ion exchange. *Separ. Sci. Technol.*
343 45, 762-767.
- 344 • Chaplin, B.P., Wyle, I., Zeng, H., Carlisle, J.A., Farrell, J., 2011. Characterization of
345 the performance and failure mechanisms of boron-doped ultrananocrystalline
346 diamond electrodes. *J. Appl. Electrochem.* 41, 1329-1340.
- 347 • Cornelis, C., D'Hollander, W., Roosens, L., Covaci, A., Smolders, R., Van Den
348 Heuvel, R., Govarts, E., Van Campenhout, K., Reynders, H., Bervoets, L., 2012.
349 First assessment of population exposure to perfluorinated compounds in Flanders,
350 Belgium. *Chemosphere* 86, 308–314.
- 351 • Directive 2013/39/EU of the European Parliament and of the Council of 12 August
352 2013 amending Directives 2000/60/EC and 2008/105/EC as regards priority
353 substances in the field of water policy. *Off. J. Eur. Union*, L 226/1, pp. 01-17 (24-
354 08-2013).
- 355 • ECHA, European Chemical Agency, 2013. Candidate list of substances of very high
356 concern for authorization. Available: [http://echa.europa.eu/web/guest/candidate-list-](http://echa.europa.eu/web/guest/candidate-list-table)
357 [table](http://echa.europa.eu/web/guest/candidate-list-table) Accessed January 22, 2014.
- 358 • Environmental Protection Agency (EPA), 2011. Drinking Water: Regulatory
359 determination on perchlorate, *Federal Register*, Volume 76 (9).
- 360 • Eschauzier, C., Beerendonk, E., Scholte-Veenendaal, P., De Voogt, P., 2012. Impact
361 of treatment processes on the removal of perfluoroalkyl acids from the drinking
362 water production chain. *Environ. Sci. Technol.* 46, 1708–1715.
- 363 • Fryda, M., Matthée, T., Mulcahy, S., Hampel, A., Schäfer, L., Tröster, I., 2003.
364 Fabrication and application of Diachem® electrodes. *Diam. Relat. Mater.* 12, 1950-
365 1956.

- 366 • Gruen, D.M., 2006. Electron transport and the potential of ultrananocrystalline
367 diamond as a thermoelectric material, in: Shenderova, O.A. & Gruen D.M. (Eds.)
368 Ultrananocrystalline diamond: synthesis, properties and applications, William
369 Andrew Publishing, New York, pp. 168.
- 370 • Johansson, J.H., Berger, U., Vestergren, R., Cousins, I.T., Bignert, A., Glynn, A.,
371 Darnerud, P.O., 2014. Temporal trends (1999-2010) of perfluoroalkyl acids in
372 commonly consumed food items. *Environ. Pollut.* 188, 102-108.
- 373 • Kapalka, A., Foti, G., Comminellis, C., 2008. Kinetic modelling of the
374 electrochemical mineralization of organic pollutants for wastewater treatment. *J.*
375 *Appl. Electrochem.* 38, 7-16.
- 376 • Lehmler, H. J., 2005. Synthesis of environmentally relevant fluorinated surfactants –
377 a review. *Chemosphere* 58, 1471–1496.
- 378 • Liao, Z., Farrell, J., 2009. Electrochemical oxidation of perfluorobutane sulfonate
379 using boron-doped diamond film electrodes. *J. Appl. Electrochem.* 39, 1993-1999.
- 380 • Lin, H., Niu, J., Ding, S., Zhang, L., 2012. Electrochemical degradation of
381 perfluorooctanoic acid (PFOA) by Ti/SnO₂-Sb, Ti/SnO₂-Sb/PbO₂ and Ti/SnO₂-
382 Sb/MnO₂ anodes. *Water Res.* 46, 2281-2289.
- 383 • Lin, H., Niu, J., Xu, J., Huang, H., Li, D., Yue, Z., Feng, C., 2013. Highly efficient
384 mild electrochemical mineralization of long-chain perfluorocarboxylic acids (C9-
385 C10) by Ti/SnO₂-Sb-Ce, Ti/SnO₂-Sb/Ce-PbO₂, and Ti/BDD electrodes. *Environ.*
386 *Sci. Technol.* 47, 13039-13046.
- 387 • Michaud, P.A., Panizza, M., Ouattara, L., Diaco, T., Foti, G., Comminellis, C., 2003.
388 Electrochemical oxidation of water on synthetic boron-doped diamond thin film
389 anodes. *J. Appl. Electrochem.* 33, 151-154.
- 390 • Niu, J., Lin, H., Xu, J., Wu, H., Li, Y., 2012. Electrochemical mineralization of

- 391 perfluorocarboxylic acids (PFCAs) by Ce-doped modified porous nanocrystalline
392 PbO₂ film electrode. *Environ. Sci. Technol.* 46, 10191-10198.
- 393 • Niu, J., Lin, H., Gong, C., Sun, X., 2013. Theoretical and experimental insights into
394 the electrochemical mineralization mechanism of perfluorooctanoic acid. *Environ.*
395 *Sci. Technol.* 47, 14341-14349.
- 396 • Ochiai, T., Iizuka, Y., Nakata, K., Murakami, T., Tryk, D.A., Fujishima, A., Koide,
397 Y., Morito, Y., 2011. Efficient electrochemical decomposition of
398 perfluorocarboxylic acids by the use of a boron-doped diamond electrode. *Diam.*
399 *Relat. Mater.* 20, 64-67.
- 400 • Ochoa-Herrera, V., Sierra-Alvarez, R., 2008. Removal of perfluorinated surfactants
401 by sorption onto granular activated carbon, zeolite and sludge. *Chemosphere* 72,
402 1588–1593.
- 403 • OSPAR, 2011. List of chemicals for priority action (Update 2011). OSPAR
404 Commission, Reference number 2004-12, pp., 1-6
- 405 • Pérez, G., Fernández-Alba, A.R., Urtiaga, A.M., Ortiz, I., 2010. Electro-oxidation of
406 reverse osmosis concentrates generated in tertiary water treatment. *Water Res.* 44,
407 2763-2772.
- 408 • Perry, R.H. (late editor), Green, D.W. (editor in chief), 2007. *Perry's Chemical*
409 *Engineers' Handbook*, 8th ed. McGraw-Hill, New York.
- 410 • Prevedouros, K., Cousins, I. T., Buck, R.C., Korzeniowski, S. H., 2006. Sources,
411 fate and transport of perfluorocarboxylates. *Environ. Sci. Technol.* 40, 32-44.
- 412 • Stockholm-Convention-Secretariat, 2009. Decision SC-4/17: listing of
413 perfluorooctane sulfonic acid, its salts and perfluorooctane sulfonyl fluoride.
414 Stockholm Convention Secretariat, pp. 1-4.

- 415 • Tai, C., Peng, J.-F., Liu, J.-F., Jiang, G.-B., Zou, H., 2004. Determination of
416 hydroxyl radicals in advanced oxidation processes with dimethyl sulfoxide trapping
417 and liquid chromatography. *Anal. Chim. Acta* 527, 73–80.
- 418 • Thompson, J., Eaglesham, G., Reungoat, J., Poussade, Y., Bartkow, M., Lawrence,
419 M., Mueller, J. F., 2011. Removal of PFOS, PFOA and other perfluoroalkyl acids at
420 water reclamation plants in South East Queensland Australia. *Chemosphere* 82, 9–
421 17.
- 422 • Urtiaga, A., Pérez, G., Ibáñez, R., Ortiz, I., 2013. Removal of pharmaceuticals from
423 a WWTP secondary effluent by ultrafiltration/reverse osmosis followed by
424 electrochemical oxidation of the RO concentrate. *Desalination* 331, 26-34.
- 425 • Urtiaga, A., Fernández-Castro, P., Gómez, P., Ortiz, I., 2014. Remediation of
426 wastewaters containing tetrahydrofuran, study of the electrochemical mineralization
427 on BDD electrodes. *Chem. Eng. J.* 239, 341-350.
- 428 • Vallejo, M., San Román, M.F., Irabien, A., Ortiz, I., 2013. Comparative study of the
429 destruction of polychlorinated dibenzo-p-dioxins and dibenzofurans during Fenton
430 and electrochemical oxidation of landfill leachates. *Chemosphere* 90, 132-138.
- 431 • Xiao, H., Lv, B., Zhao, G., Wang, Y., Li, M., Li, D., 2011. Hydrothermally
432 enhanced electrochemical oxidation of high concentration refractory
433 perfluorooctanoic acid. *J. Phys. Chem. A* 115, 13836-13841.
- 434 • Xiao, F., Davidsavor, K.J., Park, S., Nakayama, M., Phillips, B.R., 2012. Batch and
435 column study: sorption of perfluorinated surfactants from water and cosolvent
436 systems by Amberlite XAD resins. *J. Colloid. Interf. Sci.* 368, 505-511.
- 437 • Zhao, H., Gao, J., Zhao, G., Fan, J., Wang, Y., Wang, Y., 2013. Fabrication of novel
438 SnO₂-Sb/carbon aerogel electrode for ultrasonic electrochemical oxidation of
439 perfluorooctanoate with high catalytic efficiency. *Appl. Catal. B: Environ.* 136-137,

440 278-286.

441 • Zhuo, Q., Deng, S., Yang, B., Huang, J., Wang, B., Zhang, T., Yu, G., 2012.

442 Degradation of perfluorinated compounds on boron-doped diamond electrode.

443 *Electrochim. Acta* 77, 17-22.

444 • Zhuo, Q., Deng, S., Yang, B., Huang, J., Yu, G., 2011. Efficient electrochemical

445 oxidation of perfluorooctanoate using a Ti/SnO₂-Sb-Bi anode. *Environ. Sci. Technol.*

446 45, 2973-2979.

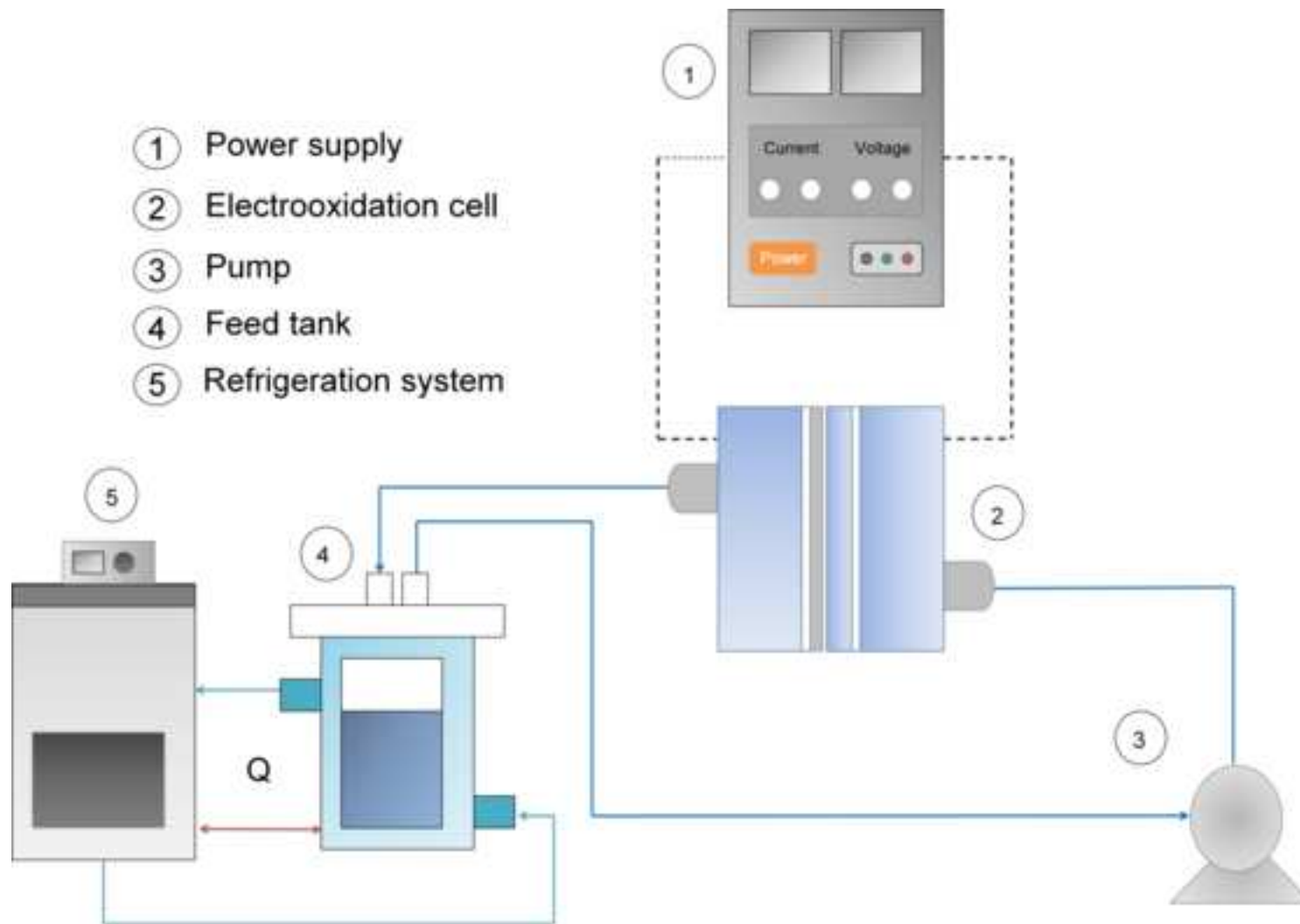
Table 1. Mineralization index at different current densities

Time (h)	M.I. (%)		
	j_{app}		
	50 A/m ²	100 A/m ²	200 A/m ²
1		57.8	93.4
2	94.9	70.6	81.8
3	87.6	68.7	83.2
4	64.2	75.4	86.1
5	77.5	77.1	85.8
6	55.8	84.1	94.9

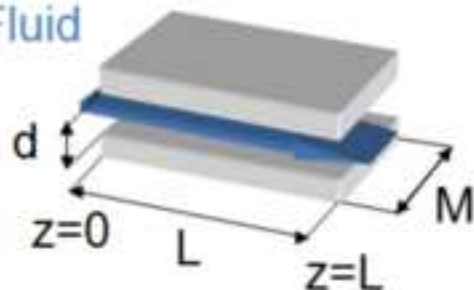
Table 2. Kinetic parameters that characterize PFOA electrochemical removal.Influence of the applied current density. PFOA 100 mg/L, T=293 K, Na₂SO₄ 5 g/L.

j_{app} (A/m ²)	Q (L/min)	Re	<i>Flow regime</i>	k_m (m/s)	$k_m(A/V)$ (s ⁻¹)	<i>Slope Fig. 5</i> (L/h)	K_c^I <i>Eq. (11)</i> (s ⁻¹)
50	6.67	3838	Turbulent	2.4×10^{-5}	2.02×10^{-4}	0.0249	2.06×10^{-4}
100						0.1101	9.10×10^{-4}
200						0.1896	15.68×10^{-4}

Figure 1



Fluid



M= electrode width, 50 mm

L= electrode length, 84 mm

d= distance between electrodes 8 mm

Figure 2

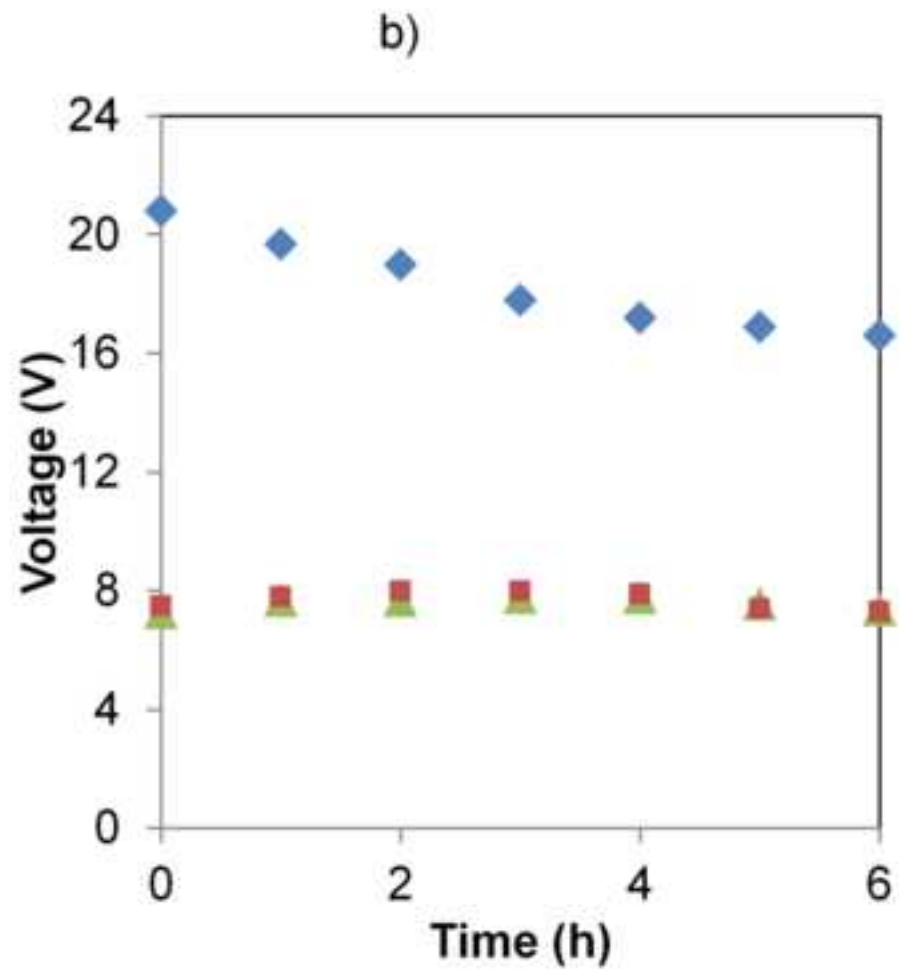
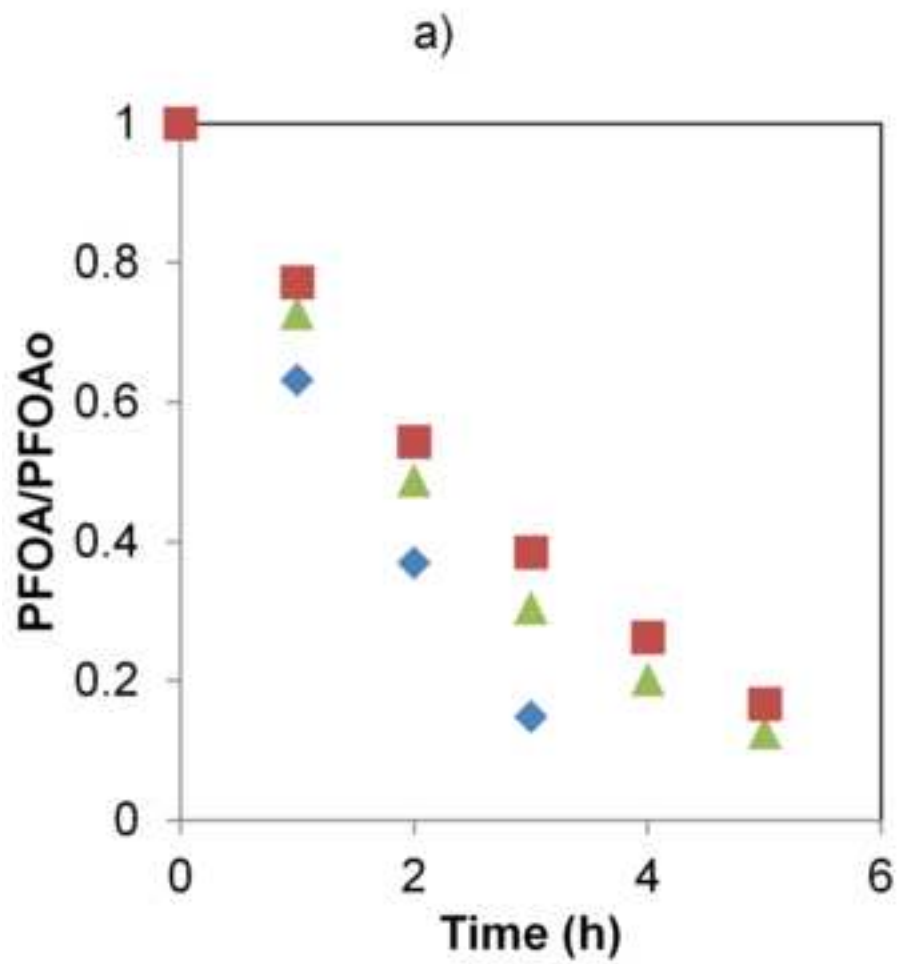


Figure 3

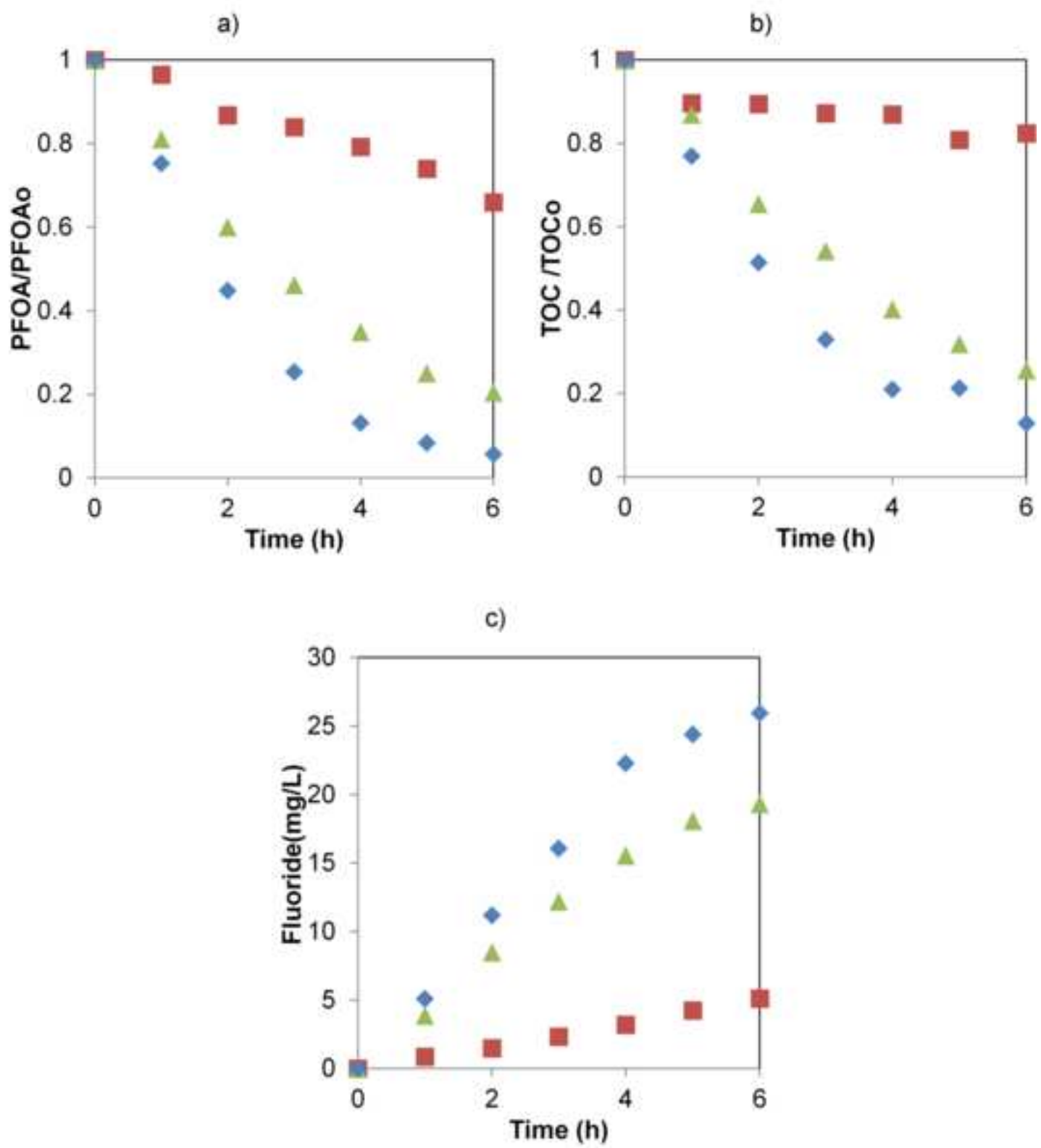


Figure 4

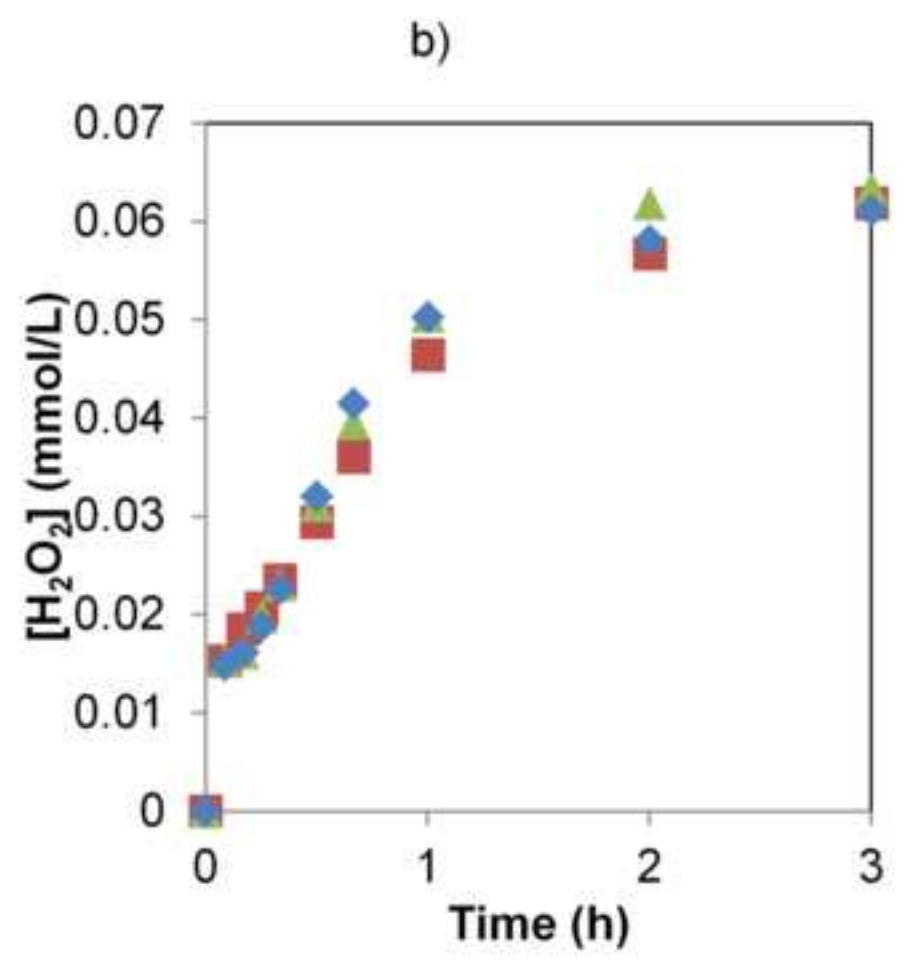
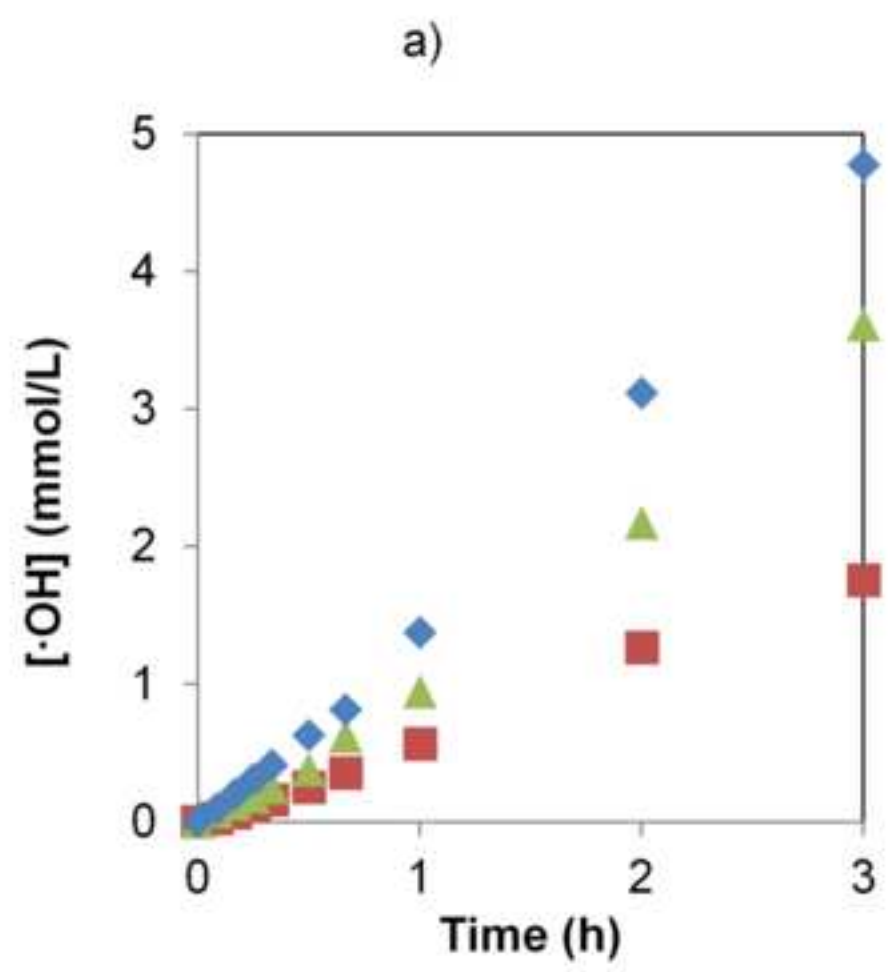


Figure 5

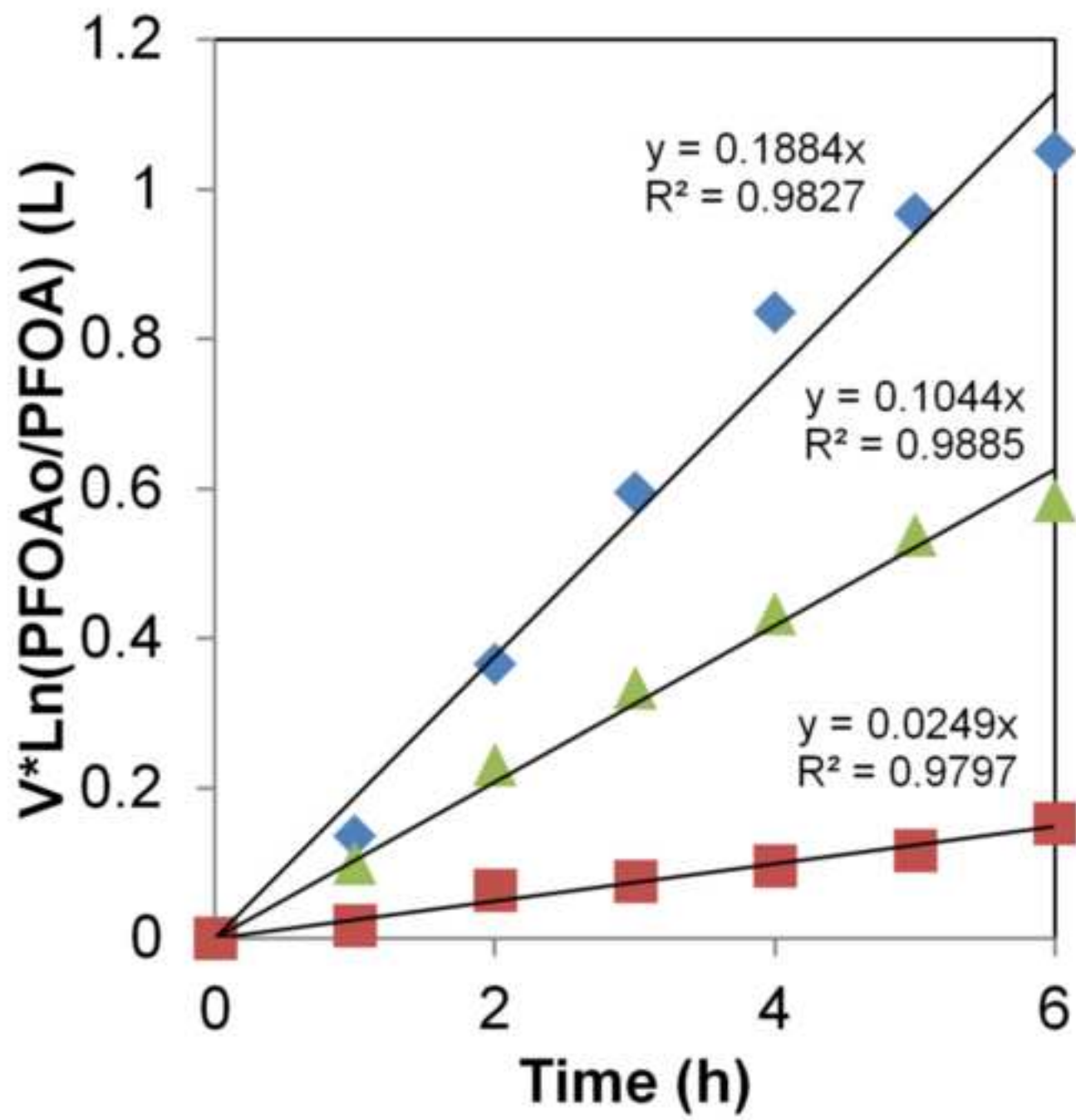


Fig. 1. Flow sheet of the experimental system used for the electro-oxidation of PFOA and detail of the electrochemical cell geometry.

Fig. 2. Influence of the electrolyte (a) on PFOA degradation rate; (b) on the cell voltage. (♦) NaClO₄, 1.4 g/L; (▲) NaClO₄, 8.4 g/L and (■) Na₂SO₄, 5 g/L. T 293 K, j_{app} 200 A/m², PFOA₀ 100 mg/L.

Fig. 3. Effect of the applied current density on the evolution of (a) PFOA concentration, (b) TOC and (c) Fluoride concentration. (■) $j_{app} = 50$ A/m², (▲) $j_{app} = 100$ A/m², (♦) $j_{app} = 200$ A/m². PFOA₀ 100 mg/L, T 293 K, Na₂SO₄ 5 g/L.

Fig. 4. Electrolysis on UNCD anodes of the electrolyte Na₂SO₄ 5 g/L, DMSO 250 mol/m³, T 293 K at different current densities: (■) $j_{app} = 50$ A/m², (▲) $j_{app} = 100$ A/m², (♦) $j_{app} = 200$ A/m². (a) Generation of hydroxyl radicals (b) Generation of hydrogen peroxide.

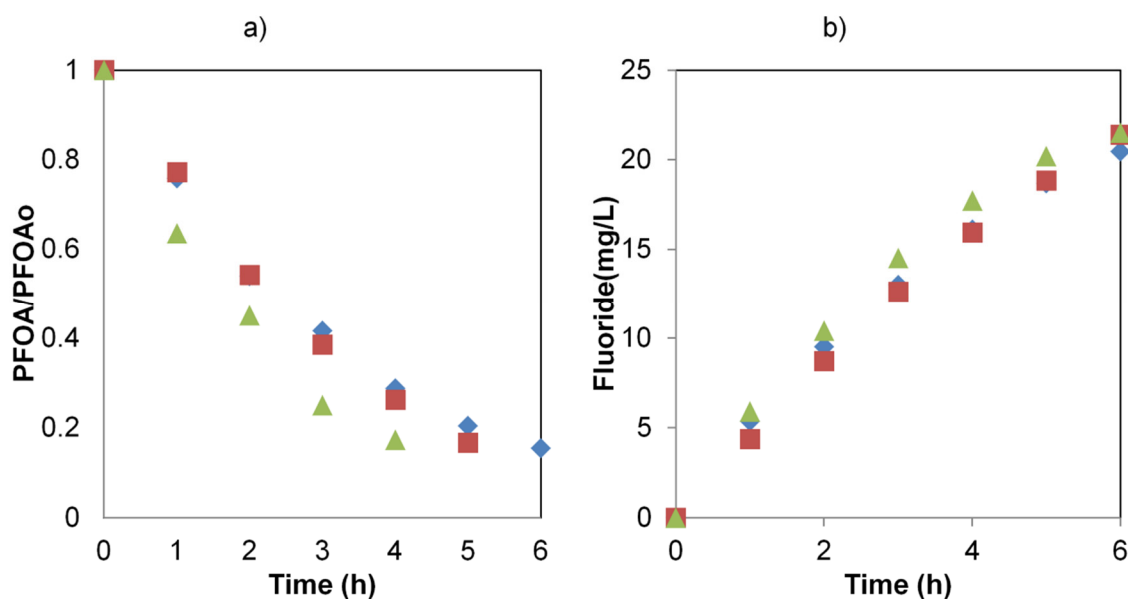
Fig. 5. Fitting of experimental data of PFOA degradation to the kinetic model, Eq. (11) (♦) j_{app} 200 A/m²; (▲) j_{app} 100 A/m²; (■) j_{app} 50 A/m²

Fig. SM-1. Influence of the flowrate on the electrooxidation of PFOA: (♦) 0.4×10^{-4} m³/s; (■) 1.11×10^{-4} ; (▲) 1.7×10^{-4} m³/s. PFOA₀ 100 mg/L, $j_{app}=200$ A/m², T 293 K, Na₂SO₄ 5 g/L.

Fig. SM-2. Influence of the temperature on the electrooxidation of PFOA: (■) 293 K; (♦) 303 K; (▲) 313 K. Experimental conditions: j_{app} 200 A/m², Na₂SO₄ 5 g/L.

1

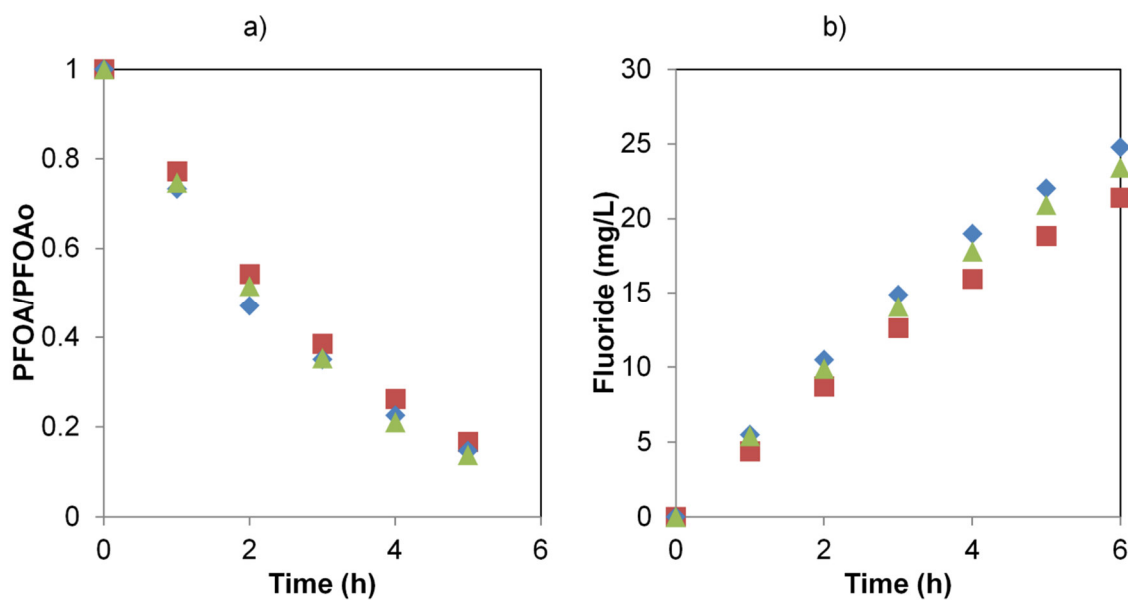
SUPPLEMENTARY MATERIAL



2

3 **Fig. SM-1.** Influence of the flowrate on the electro-oxidation of PFOA: (♦) 0.4×10^{-4}
 4 m^3/s ; (■) 1.11×10^{-4} ; (▲) $1.7 \times 10^{-4} \text{m}^3/\text{s}$. PFOA₀ 100 mg/L, $j_{app}=200 \text{ A}/\text{m}^2$, T 293 K,
 5 Na₂SO₄ 5 g/L.

6

7
8

9 **Fig. SM-2.** Influence of the temperature on the electro-oxidation of PFOA: (■) 293 K;
 10 (♦) 303 K; (▲) 313 K. Experimental conditions: $j_{app} 200 \text{ A}/\text{m}^2$, Na₂SO₄ 5 g/L.